Article

Not peer-reviewed version

Identification of EGF Receptor and Thrombospondin-1 As En-Dogenous Targets of ER-Associated Degradation Enhancer EDEM1 in HeLa Cells

Kohta Miura , Riko Katsuki , Shusei Yoshida , Ren Ohta , Taku Tamura *

Posted Date: 12 June 2023

doi: 10.20944/preprints202306.0751.v1

Keywords: Endoplasmic reticulum-associated degradation (ERAD); EDEM1; ER chaperone; EGF receptor; TSP1

Article

Identification of EGF Receptor and Thrombospondin-1 as Endogenous Targets of ER-Associated Degradation Enhancer EDEM1 in HeLa Cells

Kohta Miura [1], Riko Katsuki [1], Shusei Yoshida [2], Ren Ohta [1] and Taku Tamura [1,2,*]

[1] Department of Life Science, Graduate School of Engineering Science, Akita University, Japan.
[2] Department of Life Science, Faculty of Engineering Science, Akita University, Akita, Japan.
* Correspondence: Taku Tamura: Department of Life Science, Faculty of Engineering Science, Akita University, 1-1 Tegata Gakuenmachi, Akita, 010-8502, Japan. Tel: +81-18-889-2377, Email: taku@gipc.akita-u.ac.jp

Abstract: Secretory and membrane proteins are vital for cell activities, including intra- and intercellular communication. Therefore, protein quality control in the endoplasmic reticulum (ER) is an essential and crucial process for eukaryotic cells. Endoplasmic reticulum-associated degradation (ERAD) targets misfolded proteins during the protein maturation process in the ER and leads to their disposal. This process maintains the ER productive function and prevents misfolded protein stress (i.e., ER stress). The ERAD-stimulating factor ER degradation-enhancing α mannosidase-like 1 protein (EDEM1) acts on misfolded proteins to accelerate ERAD, thereby maintaining the productivity of the ER. However, the detail mechanism underlying the function of EDEM1 in ERAD is not completely understood due to lack of established physiological substrate proteins. In this study, we attempted to identify substrate proteins for EDEM1 using siRNA. The matrix component thrombospondin-1 (TSP1) and epidermal growth factor receptor (EGFR) were identified as candidate targets of EDEM1. Their protein maturation status and cellular localization were markedly affected by knockdown of EDEM1. We also showed that EDEM1 physically associates with EGFR and enhances EGFR degradation via ERAD. Our data highlight the physiological role of EDEM1 in maintaining specific target proteins and provide a potential approach to the regulation of expression of clinically important proteins.

Keywords: endoplasmic reticulum-associated degradation (ERAD); EDEM1; ER chaperone; EGF receptor; TSP1

1. Introduction

In eukaryotes, secretory and membrane proteins are important for a variety of intra- and intercellular events. Endoplasmic reticulum (ER) is the organelle involved in the production of secretory and membrane proteins. In the ER, organized protein quality control systems, productive protein folding, and selective degradation of misfolded proteins are executed. Protein folding and assembly in the ER are assisted by ER-resident chaperones, disulfide bond-producing enzymes, and N-linked glycan modification enzymes. Moreover, terminally misfolded or unassembled proteins are disposed through a process termed ER-associated degradation or ERAD. These processes, which complement each other, are termed ER quality control systems (ERQC) [1]. Co- and post-translational N-glycosylation, as well as its trimming, are vital signs for protein maturation and ERAD [2,3]. As protein biosynthesis proceeds, mannose residues of N-glycan on glycoproteins are removed and act as an ERAD indicator in the ER [4]. The ER is a membrane-surrounded tubule structure filled with various proteins. Thus, maturation of newly translated proteins is a complicated process, leading to failed protein products. Exceeding the capacity of ERAD causes accumulation of misfolded proteins at the ER and triggers stress responses. This process results in the production of folding support proteins (e.g., molecular chaperones or modifying enzymes, ERAD-related factors), and finally leads to apoptosis [5].

 doi:10.20944/preprints202306.0751.v1

Recent studies on ERQC have highlighted the physiological importance of ERAD. Regulation of protein turnover by ERAD is required for cellular development and physiological balances [6,7]. The SEL1L/Hrd1 complex is a central mechanism of ERAD where misfolded proteins are gathered, retro-translocated to the cytoplasm, and polyubiquitylated for proteasomal degradation [8]. It has been shown that the SEL1L/Hrd1 complex is required for various life events and cellular functions, including development and growth regulation of the liver [9–11]. OS-9, which recognizes 5–6 mannose N-glycan of ERAD substrates and acts as a downstream factor of SEL1L/Hrd1 ERAD pathway, targets CD147 and the Na-K-2Cl co-transporter NKCC2 [3,12,13]. Recent proteomic investigations uncovered endogenous substrates of specific ERAD factors and allowed the elucidation of the detailed mechanism underlying their interaction with target proteins [14,15]. Thus, the identification of endogenous target proteins for ERAD in tissues or in developmental stages extend the role and function of protein degradation in physiology and development.

EDEM1, an ER-associated degradation enhancing alpha mannosidase-like factor 1, is a ERAD-enhancing factor that facilitates the clearance of various ERAD model proteins [16]. It has been demonstrated that EDEM1 accelerates several steps of ERAD. EDEM1 exhibits mannose trimming activity of N-glycans and presents misfolded proteins following interaction with downstream ERAD factors, such as OS-9 and XTP3B [17–19]. During ERAD acceleration, EDEM1 selectively binds to immature proteins which contain free-thiol or a hydrophobic region exposed at the molecular surface [19,20]. Furthermore, the mannosidase-like domain of EDEM1 is required for association with SEL1L in a mannose trimming-dependent manner, suggesting that the role of EDEM1 in ERAD is to present substrate misfolded proteins to the SEL1L/Hrd1 complex [20]. In addition, EDEM1 interacts with transmembrane-form and soluble ERAD substrates, as well as ERAD-related cellular factors [21]. This is achieved by creating both soluble and transmembrane forms of EDEM1 through slow signal sequence cleavage [21]. However, the physiological significance of EDEM1 and EDEM1-mediated ERAD remains unclear owing to the lack of information on the targets of EDEM1.

In this study, we attempted to identify endogenous substrates of EDEM1 and explored their role in ERAD. Downregulation of EDEM1 gene expression by siRNA induced the accumulation of certain ER-resident chaperones. This finding suggested that inhibition of EDEM1-mediated ERAD causes accumulation of misfolded proteins in the ER. We ascertained that thrombospondin-1 (TSP1) and epidermal growth factor receptor (EGFR) are endogenous targets of EDEM1 for ERAD in HeLa cells. Furthermore, we characterized their degradation under basal state and EDEM1-knockdown (KD) conditions. We found that their cellular location and folding status were affected by EDEM1-mediated ERAD. We also revealed that EDEM1 associates with EGFR and enhances the degradation of EGFR that is inhibited by the proteasome inhibitor, MG132. These data suggested that ERAD is involved in EGFR turnover. Collectively, our results suggest that basal expression of EDEM1 is required for maintaining the productivity of the ER through the downregulation of misfolded ER proteins, including TSP1 and EGFR.

2. Results

2.1. Downregulation of EDEM1 gene expression induced ER stress and apoptosis

It is well established that the protein expression levels of EDEM1 greatly affect the disposal of misfolded ER proteins through ERAD. EDEM1 gene expression is upregulated by ER stress in which unfolded protein responses (UPR) restrict the production of secretory and membrane proteins and activate ERAD. However, the activity and role of EDEM1 in cells with low ER stress is not well understood. To explore the function of EDEM1 at basal levels, we performed transient mRNA downregulation of EDEM1 using siRNA. The EDEM1 mRNA levels were clearly decreased compared with those of the housekeeping gene glyceraldehyde-3-phosphate dehydrogenase (GAPDH) (Figure 1A). Moreover, it was found that the gene expression levels of the spliced form of XBP1 (XBP1s), an ER stress marker and transcription factor involved in UPR, were markedly enhanced by EDEM1 KD (Figure 1A). We examined whether EDEM1 KD by siRNA is applicable to exogenously expressed ERAD substrates null Hong Kong alpha1 antitrypsin (NHK) and CD10 C143Y

 doi:10.20944/preprints202306.0751.v1

[22]. The degradation of both ERAD substrates was suppressed or even aggregated by siRNA for EDEM1 (Figure S1), indicating that our experimental condition is effective in HeLa cells. When the treatment with siRNA for EDEM1 was extended up to 96 h, the protein expression of CCAAT-enhancer-binding protein homologous protein (CHOP) (an UPR marker that stimulates ER stress-mediated apoptosis [23]) was upregulated (Figure 1B). Moreover, typical morphological features of apoptosis, such as cell shrinkage and nuclear fragmentation, were also observed (Figure 1C). Consequently, these results suggest that the functions of EDEM1 (even at basal levels) are to maintain the ERQC and prevent ER stress by ERAD of misfolded proteins.

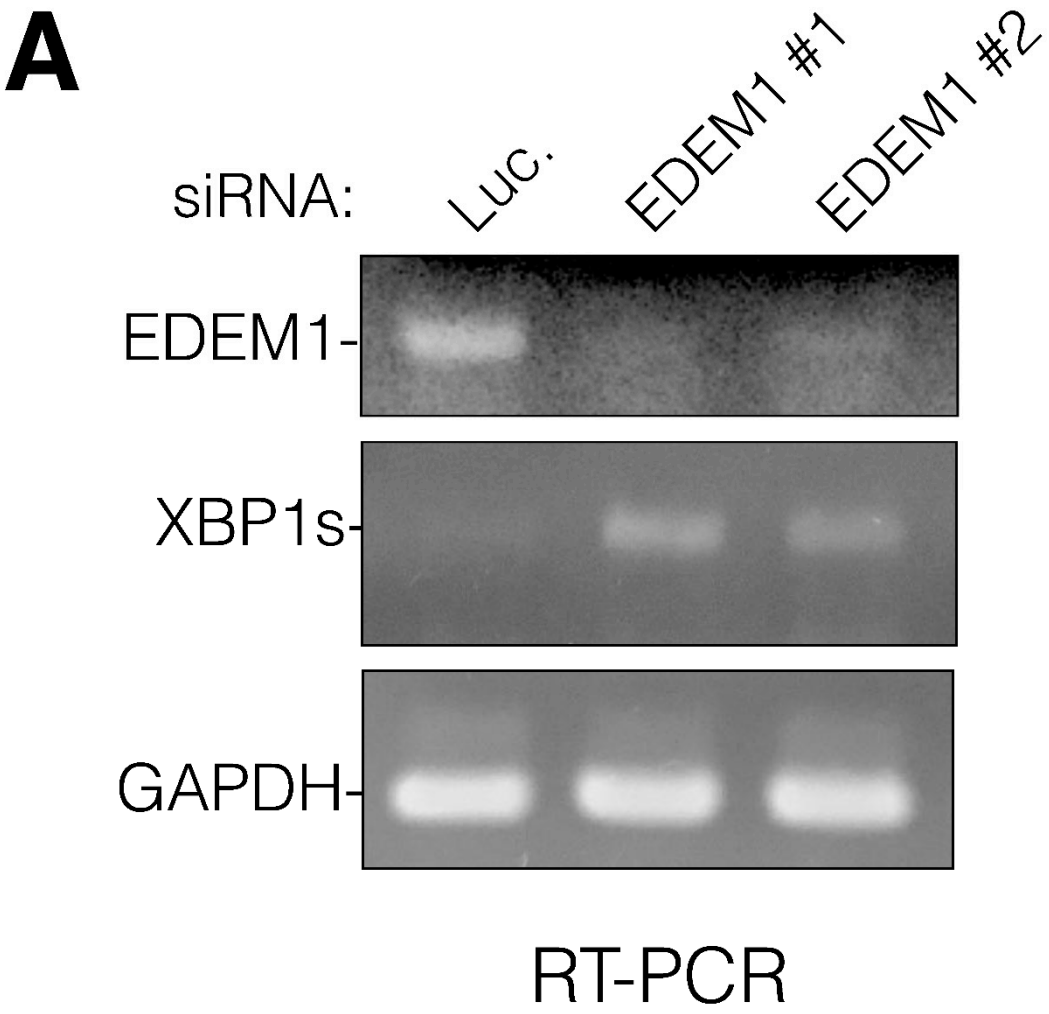

 doi:10.20944/preprints202306.0751.v1

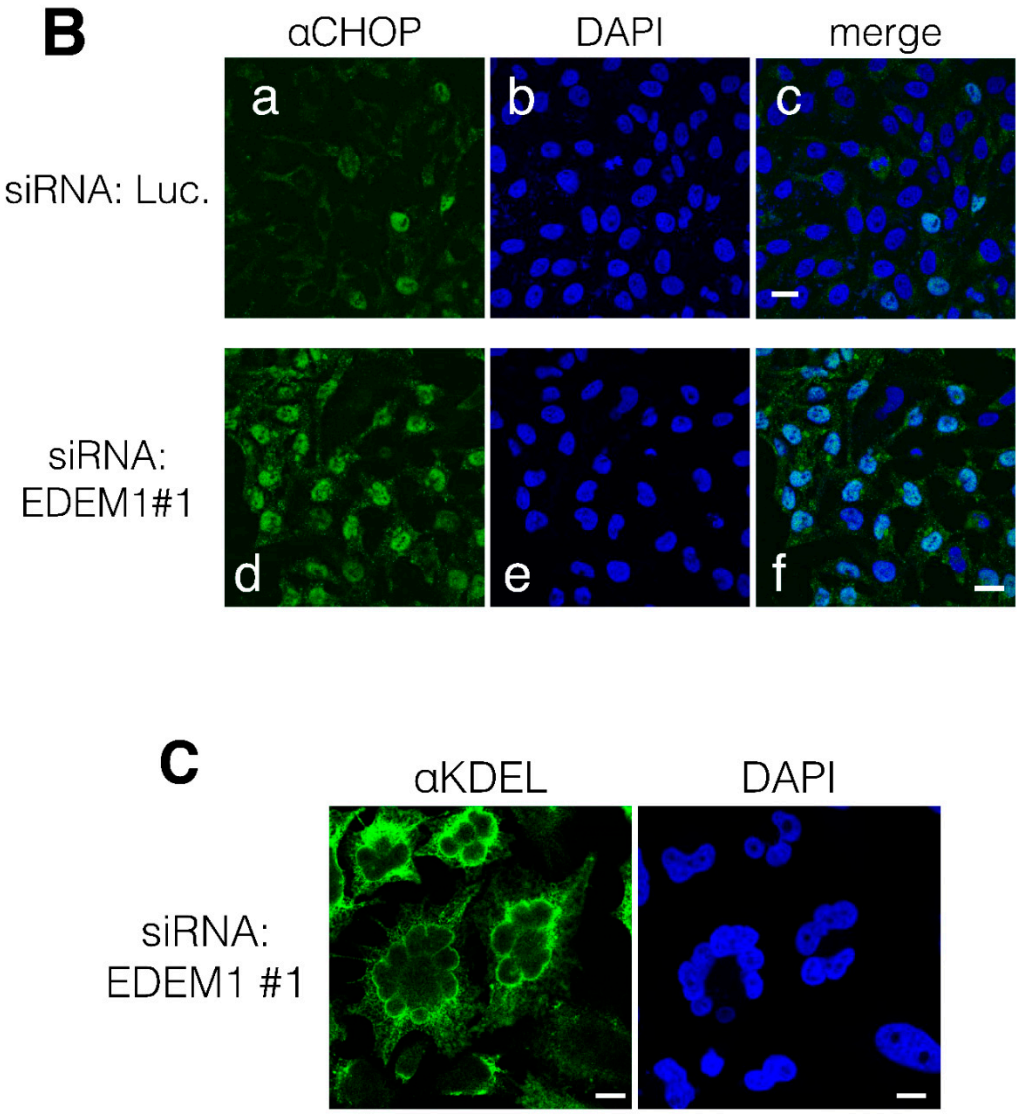

Figure 1. siRNA-mediated mRNA downregulation of EDEM1 caused ER stress and apoptosis. Knockdown of EDEM1 gene by siRNA upregulated the UPR and induced apoptosis in HeLa cells. (**A**) After treatment with indicated siRNA (luciferase [Luc.]), EDEM1#1 and EDEM1#2 for 72 h), HeLa cells were lysed, and mRNA samples were prepared as described in the Materials and Methods section. The mRNA of EDEM1, XBP1s, and GAPDH of control cells (Luc.) and EDEM1 KD cells was amplified and detected by agarose gel electrophoresis. (**B**) After 72 h of siRNA treatment, HeLa cells were fixed with paraformaldehyde and immunodetected using an anti-CHOP antibody (an ER stress marker associated with apoptosis). Scale bars in panel c and f represent 10 μm. (**C**) After 96 h of siRNA treatment, HeLa cells were fixed and immunodetected using an anti-KDEL antibody which recognizes ER-resident KDEL sequence-containing proteins. Scale bar represents 10 μm.

2.2. ER chaperone clustering by EDEM1 siRNA KD

Indirect immunostaining using antibodies against ER-resident proteins was conducted to visualize the effect of EDEM1 KD on ER morphology. A soluble ER heat shock protein 70 (HSP70) family chaperone binding immunoglobulin protein (BiP) exhibited as an ER network structure under siRNA to luciferase as a negative control (Figure 2). However, after EDEM1 KD, BiP appeared as punctuated structures (Figure 2). Such morphological change was also observed for ERp19, one of the protein disulfide isomerase-family (PDI-family) proteins that assists in disulfide bond formation of ER-folding proteins [24] (Figure 2). Indirect immunostaining using an anti-KDEL antibody, which

 doi:10.20944/preprints202306.0751.v1

recognizes proteins bearing the C-term KDEL sequence, such as BiP, calreticulin (CRT), PDI, and ERp57, exhibited punctuated structures similar to those noted with anti-BiP (Figure S2). This result suggests that misfolded proteins destined for ERAD were assembled following EDEM1 KD and caused the accumulation of the above ER chaperones. Interestingly, calnexin (CNX), a membrane-anchored homolog of CRT, and UDP-glucose:glycoprotein glucosyltransferase 1 (UGGT1) did not form a cluster after EDEM1 KD (Figure S2). Our morphological analyses suggested that EDEM1 targets misfolded proteins after the CNX cycle and proteins with insufficient disulfide bonds. UGGT1 recognizes immature glycoproteins and acts as a gatekeeper of ER glycoproteins to add monoglucose to the N-glycan of immature proteins for re-entry into the CNX cycle [25]. The differences in the obtained immunostaining observations may result from the distinction between two ER protein-folding mechanisms, namely CNX-UGGT1 and CRT-ERp57-BiP; the former targets newly synthesized proteins, while the latter targets relatively misfolded proteins.

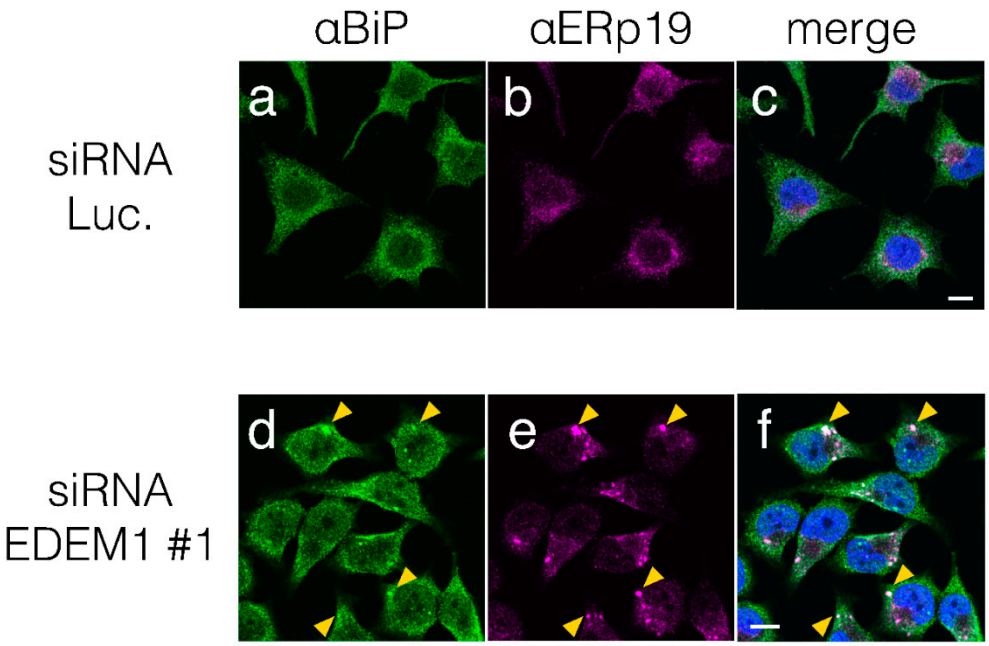

Figure 2. EDEM1 KD induced ER chaperone accumulation. Treatment with EDEM1 siRNA induced the accumulation of some ER-resident chaperones in HeLa cells. (**A**) After control (Luc., a–c) or EDEM1#1 (d–f) siRNA treatment, ER chaperone proteins BiP (a and d) and ERp19 (b and e) were immunodetected using corresponding antibodies. Merged images after DAPI staining are also shown (c and f). Some co-localization points in panels d–f are indicated by yellow triangles. Scale bars in panel c and f represent 10 μm.

2.3. EDEM1 KD resulted in ER accumulation of TSP1

Next, we sought to understand the importance of EDEM1 in cell viability. Therefore, we explored secretory or membrane proteins that are degraded by EDEM1-mediated ERAD. Such proteins may accumulate in the ER by EDEM1 KD probably due to insufficient disposal from the ER and aggregate owing to the hydrophobicity of the molecules. Through biochemical analysis, the secretory protein TSP1 and the single transmembrane protein EGFR were identified as the endogenous substrate proteins of EDEM1 for ERAD. TSP1 is a soluble extracellular matrix protein that mediates intercellular connection through heparin binding and an EGF-like module [26]. Post-translational modifications of TSP1, including several disulfide bonds and N-glycans, are important for its structural stability and function [27]. Indirect immunostaining showed that, in terms of intracellular location, TSP1 exhibited an ER-like pattern and showed similar distribution to ERp57 (Figure 3A, a–c). Following EDEM1 gene suppression, ERp57 exhibited similar clustering to that

 doi:10.20944/preprints202306.0751.v1

observed for BiP and ERp19 (see Figure 2A, d). Notably, some punctuations of TSP1 were colocalized with ERp57 (Figure 3A, d–f). These results suggested that the EDEM1-mediated ERAD could remove misfolded TSP1 from the ER. To further characterize the protein aggregation status, we biochemically analyzed intracellular TSP1 under EDEM1 gene KD condition. Misfolded proteins tend to expose the hydrophobic region to the molecular surface of the proteins. Thus, the detergent-insoluble fraction of the cell lysate was analyzed to evaluate the folding status. KD of EDEM1 increased the insoluble fraction of TSP1 (Figs. 3B and C). These results are consistent with those obtained from the indirect immunostaining assay that showed punctuation of TSP1. These findings suggested that ERAD by EDEM1 is important for the clearance of misfolded TSP1 molecules from the ER.

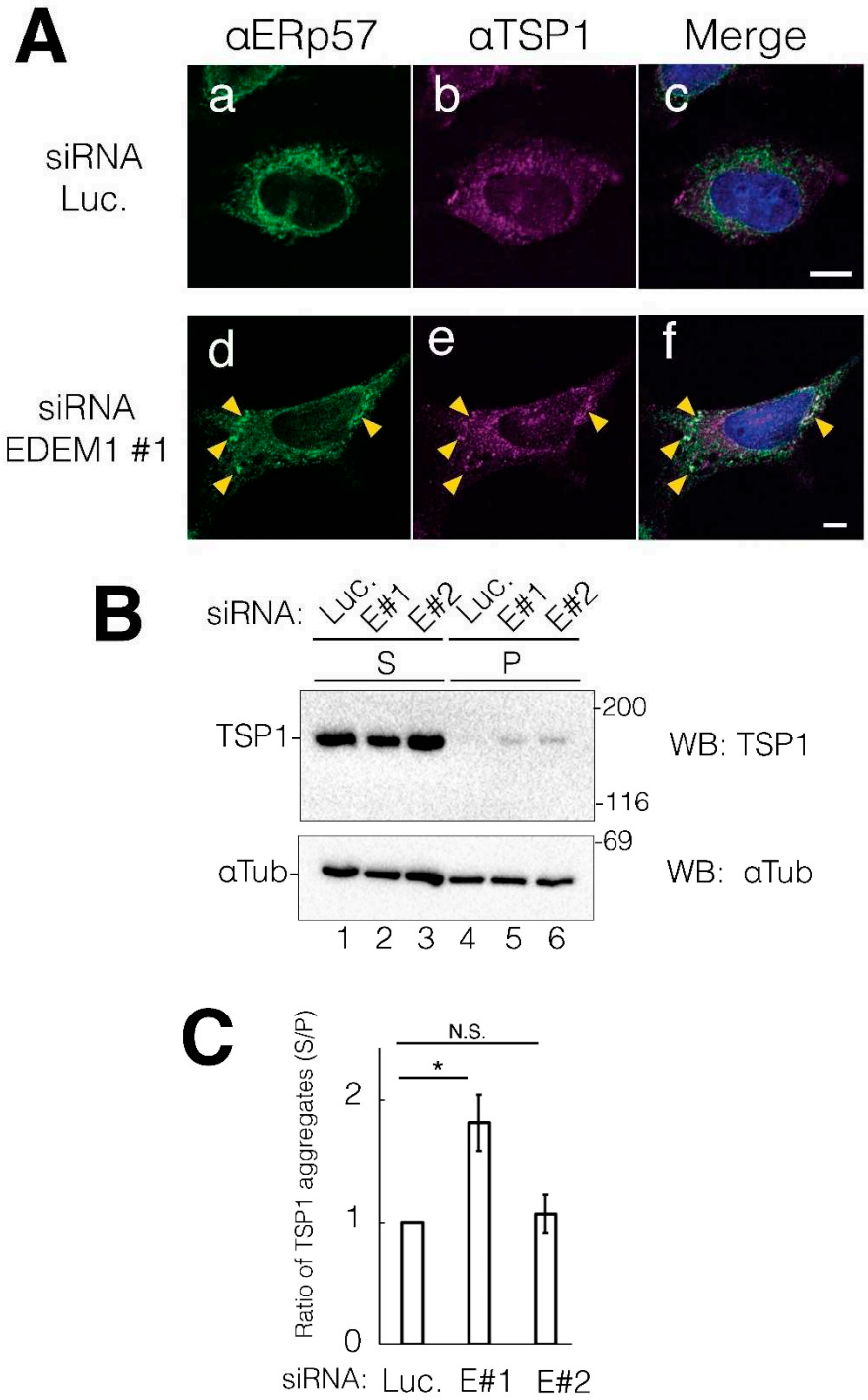

Figure 3. Downregulation of EDEM1 induced intracellular aggregation of TSP1. EDEM1 KD led to the accumulation of the matrix soluble protein TSP1 in cells. (**A**) After control or EDEM1#1 siRNA

 doi:10.20944/preprints202306.0751.v1

treatment, ER-resident chaperone ERp57 (a and d) and TSP1 (b and e) were immunodetected using corresponding antibodies. Merged images after DAPI staining are also shown (c and f). Co-localization points of ERp57 and TSP1 in EDEM1 KD cells are indicated by yellow triangles (d–f). Scale bars represent 10 μm. (**B**) siRNA-treated cells were lysed and separated into soluble supernatant (S) and insoluble precipitation (P) fractions. Both TSP1 and αTubulin were detected by western blotting with indicated antibodies for control (lanes 1 and 4) and EDEM1 KD cells (lanes 2 and 5, 3 and 6). Lane numbers are shown at the bottom of the gel. The molecular weight of marker proteins (kDa) is shown at the right side of the gel. (**C**) Data in (B) were quantified. αTubulin was used as the cellular loading control. In each sample set (lanes 1 and 4, 2 and 5, 3 and 6, respectively), the values of anti-Flag bands were normalized to those of anti-αTubulin. Notably, the values of soluble bands were normalized to those of precipitation bands. Asterisks refer to the control sample, indicating statistical significance (*$p < 0.05$; N.S., not significant) according to Student's *t*-test. Data represent the mean ± standard deviation of three independent experiments.

2.4. EDEM1 KD induced EGFR accumulation in ER

EGFR directs cell proliferation through EGF-mediated extracellular signaling. In addition, it is regarded as an oncogene and its gene expression is upregulated in various types of cancer [28]. Since EGFR contains numerous disulfide bonds and N-linked glycans, we tested whether EGFR is a target of EDEM1 for ERAD. EGFR was almost undetectable in the detergent-insoluble fraction under the negative control siRNA. These data suggested that endogenous EGFR is properly folded and misfolded EGFR is degraded smoothly in HeLa cells (Figure 4A, lane 4). However, detergent-insoluble EGFR was detected after EDEM1 KD (Figure 4A, lanes 5 and 6). The amount of aggregated EGFR was correlated with the efficacy of EDEM1 KD (comparing #1 and #2. See Figure 1), indicating that EDEM1 works for the disposal of misfolded EGFR during its folding in the ER (Figure 4B).

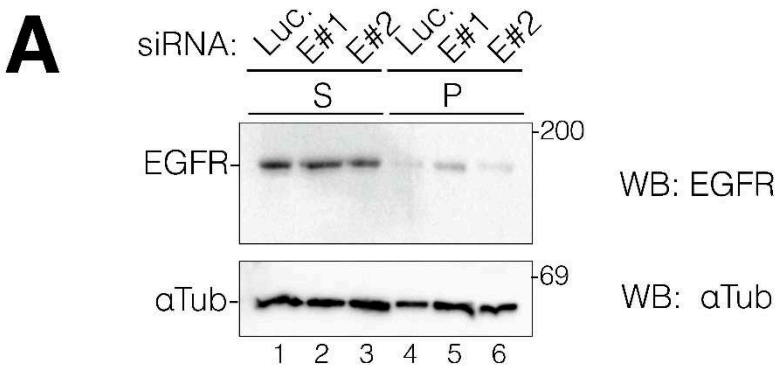

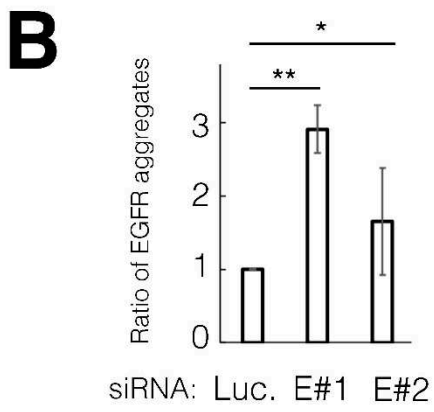

 doi:10.20944/preprints202306.0751.v1

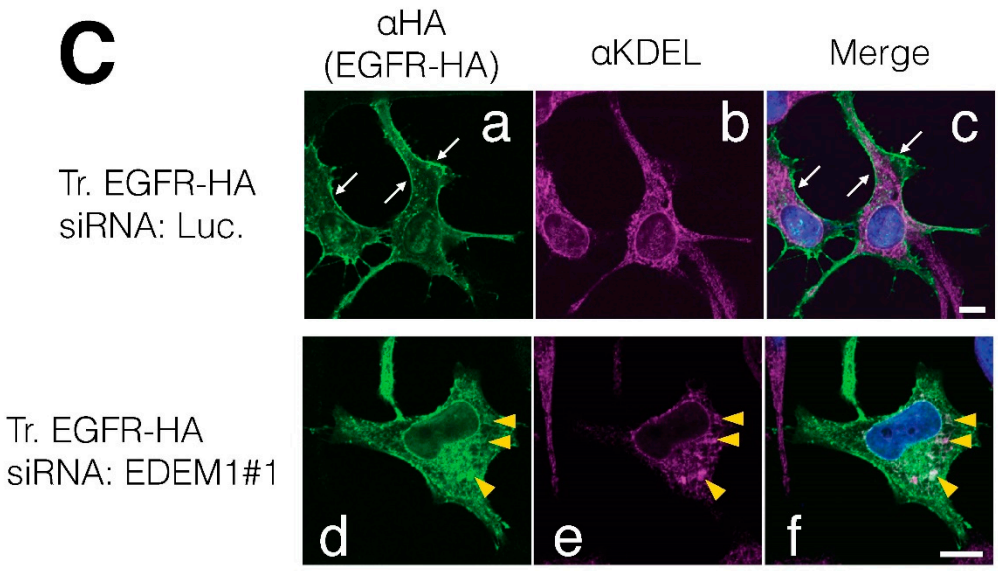

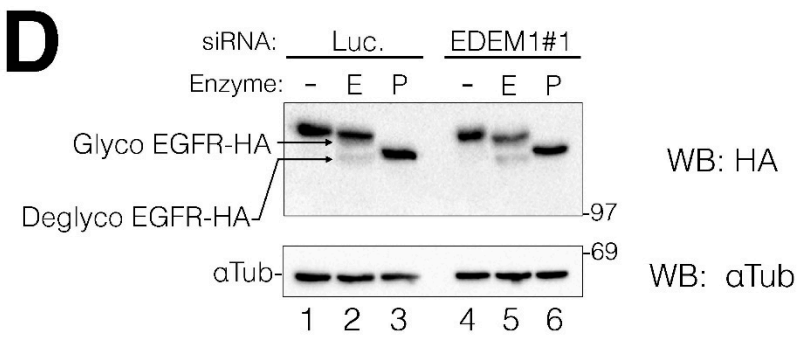

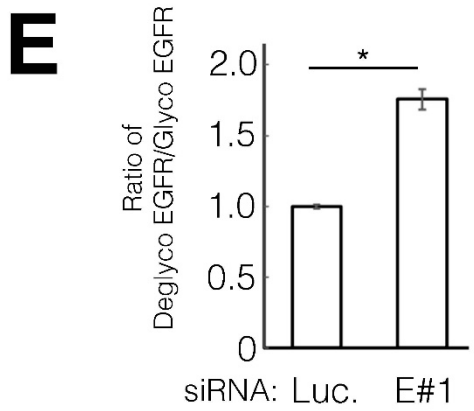

Figure 4. EDEM1 knockdown (KD) increased the detergent-insoluble and intracellular EGFR fractions. EDEM1 KD affected the cellular localization and protein solubility of EGFR. (**A**) siRNA-treated cells were lysed and fractionated into detergent-soluble (S) and -insoluble fractions (P). Protein bands of EGFR and αTubulin were immunodecorated with indicated antibodies for control (lanes 1 and 4) and EDEM1 KD (lanes 2 and 5, 3 and 6). Lane numbers are shown at the bottom of the gel. The molecular weight of marker proteins (kDa) is shown at the right side of the gel. (**B**) Quantification of (A). αTubulin was used as the cellular loading control. In each sample set, (lanes 1 and 4, 2 and 5, 3 and 6, respectively), the values of anti-Flag bands were normalized to those of anti-αTubulin. Of note, the values of soluble bands were normalized to those of precipitation bands. Asterisks refer to the control sample, indicating statistical significance (*$p < 0.05$; **$p < 0.01$) by

Student's *t*-test. Data represent the mean ± standard deviation of three independent experiments. (**C**) During siRNA treatment with control (a–c) or EDEM1#1 (d–f), cells were transfected with EGFR-HA, and cellular localization was verified by indirect immunostaining. After fixation with methanol, proteins were visualized using anti-HA (EGFR-HA, green) and anti-KDEL (KDEL motif-containing proteins, magenta) antibodies. Merged images after DAPI staining are shown as c (control) and f (EDEM1#1). The co-localization of EGFR-HA and KDEL proteins is represented by yellow triangles. Scale bars in c and f represent 10 μm. (**D**) Ratio of post-Golgi and ER-retained EGFR-HA following EDEM1 KD. Denatured lysates from HeLa cells treated with control (lanes 1–3) or EDEM1#1 (lanes 4–6) siRNA were digested with mock (lanes 1 and 4), Endo H (lanes 2 and 5), and PNGase F (lanes 3 and 6). The positions of N-glycosylated (Glyco EGFR-HA, post-Golgi) and deglycosylated EGFR-HA (Deglyco, ER) in SDS-PAGE are indicated at the left side of the gel. (**E**) Quantification of data from E is shown. In lanes 2 and 5, the values of deglyco EGFR-HA bands were divided by those of glyco EGFR-HA bands. The values were standardized to those of αTubulin. Asterisks refer to the control sample, indicating statistical significance (*$p < 0.05$) by Student's *t*-test. Data represent the mean ± standard deviation of three independent experiments.

To ascertain whether EDEM1 is involved in EGFR biosynthesis, we constructed hemagglutinin-tagged (HA-tagged) EGFR at the C-term (EGFR-HA). Thereafter, the intracellular trafficking of EGFR-HA during siRNA experiments was examined. Indirect immunostaining with antibodies against HA and KDEL (ER marker) showed that EGFR-HA was localized at the plasma membrane under negative control siRNA (Figure 4C, a). This result indicated that exogenously expressed EGFR-HA was properly folded in the ER and transported to the plasma membrane in HeLa cells. However, EGFR-HA was merged with anti-KDEL staining and exhibited some clusters under EDEM1 KD (Figure 4C, d-f). Furthermore, EGFR-HA staining was also showed nuclear membrane-like structures that is associated with the ER (Figure 4C, d). These results suggested that EDEM1 is involved in misfolded EGFR clearance that is retained in the ER by the ERQC. To further confirm the involvement of EDEM1 in the intracellular trafficking of EGFR-HA, we performed endoglycosidase H (Endo H) digestion of the N-glycans of EGFR-HA. Endo H treatment resulted in both slower (Endo H-resistant form) and faster (Endo H-sensitive form) migration of EGFR-HA, representing post-Golgi and ER localization, respectively. Following treatment with negative control siRNA, markedly higher levels of the Endo H-resistant form of EGFR versus the Endo H-sensitive form were detected (Figure 4D, lane 2). However, KD of EDEM1 increased the levels of Endo H-sensitive EGFR-HA (comparing lanes 2 and 5, Figure 4D). These results suggested that ERAD by EDEM1 clears ER-accumulated EGFR-HA and is important for the proper cellular localization of EGFR-HA.

2.5. EDEM1 facilitated EGFR degradation through ERAD

To ascertain whether EDEM1 participates in EGFR degradation through ERAD, EGFR-HA was co-transfected with C-terminal Flag-tagged EDEM1 and the expression levels of EGFR-HA were examined. As the levels of EDEM1-Flag were increased, the protein expression of EGFR-HA was decreased (Figs. 5A and B). We also sought to investigate whether this decrease is attributed to the enhancement of ERAD of EGFR-HA by EDEM1. Hence, proteasome activity was inhibited using MG132 during the transfection, and EGFR-HA degradation was verified. EDEM1 co-expression reduced the protein expression of EGFR-HA by approximately 50% compared with control (Figure 5C, comparing lanes 1 and 2). However, in the presence of MG132, EGFR-HA expression was recovered to approximately 75% (Figs. 5C and D). These results suggested that the effect of EDEM1-Flag overexpression on EGFR-HA downregulation is due to the upregulation of ERAD. Cell surface expression of EGFR-HA was observed following the overexpression of EDEM1-Flag (Figure S3). Thus, EDEM1 could participate in the biosynthesis of misfolded EGFR-HA, but not in that of matured EGFR-HA. We investigated the physical interaction of EDEM1-Flag with EGFR-HA by co-immunoprecipitation experiments (Figure 5E). Immunoisolation and western blotting analyses revealed that EDEM1-Flag was associated with EGFR-HA (Figure 5E, lane 8). Taken together, our results suggested that EDEM1 contributes to the turnover of ERQC substrate proteins, including TSP1 and EGFR, by ERAD to prevent ER stress in cells.

 doi:10.20944/preprints202306.0751.v1

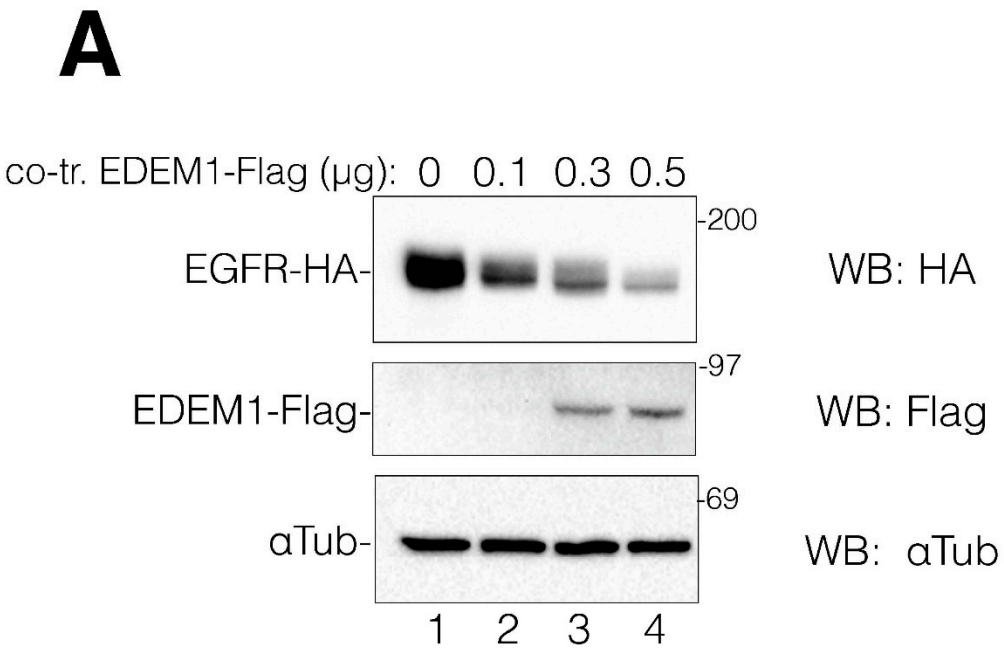

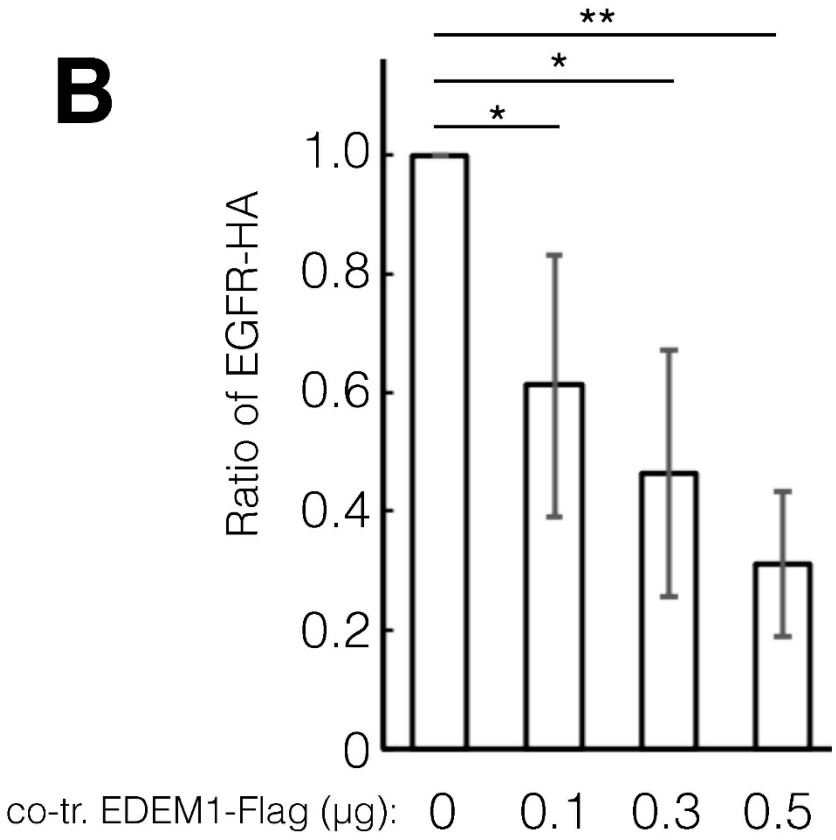

 doi:10.20944/preprints202306.0751.v1

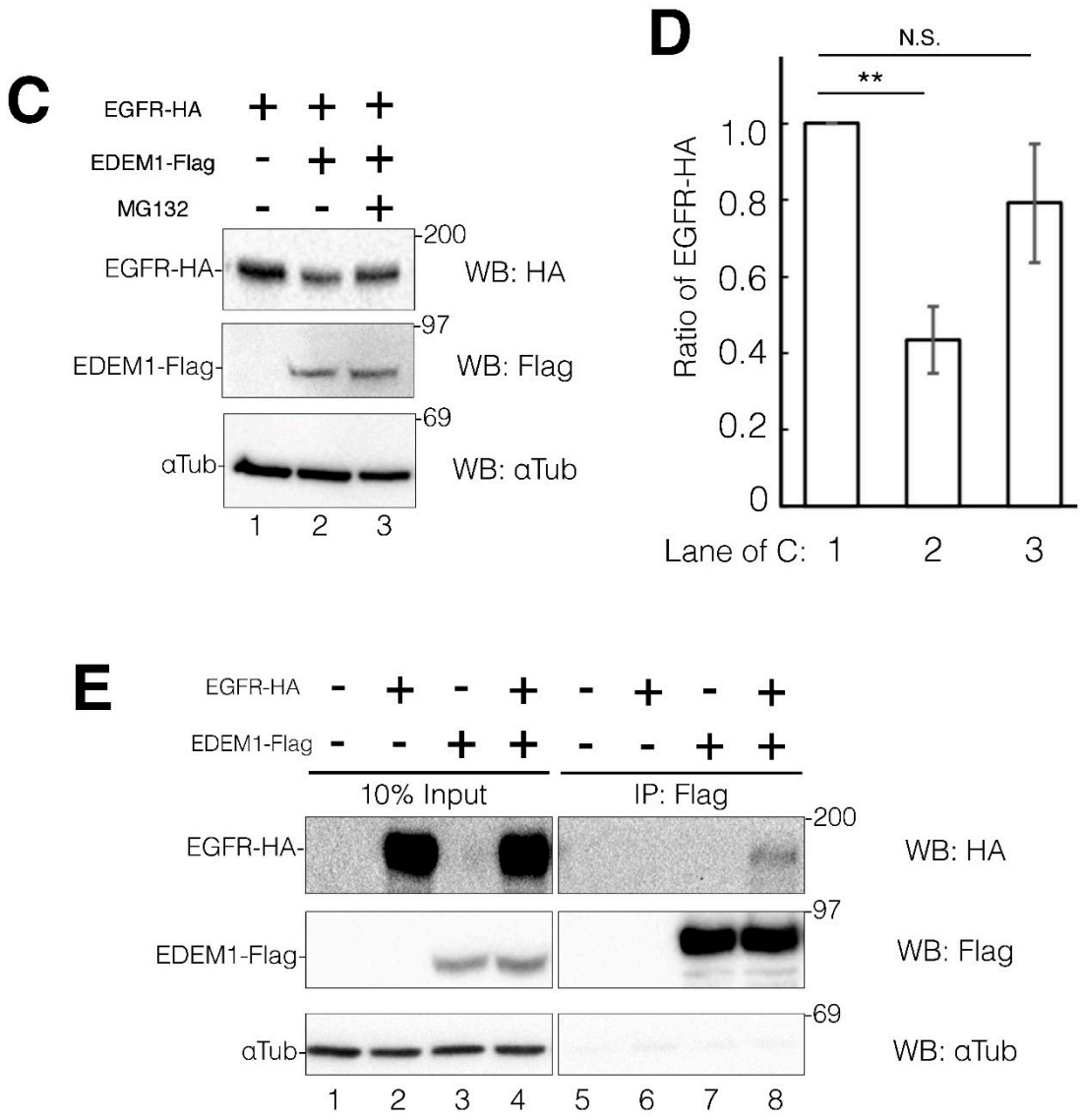

Figure 5. Co-expression of EDEM1 promoted EGFR degradation by ERAD. EGFR protein turnover is accelerated by overexpression of EDEM1 through the ERAD pathway. (**A**) Turnover of EGFR-HA is dependent on the co-expression of EDEM1-Flag. HeLa cells were transfected with a fixed amount of EGFR-HA and various EDEM1-Flag coding plasmids as indicated. Proteins were detected by western blotting using indicated antibodies. (**B**) Quantification of (A). The amount of EGFR-HA was calculated using αTubulin as a cellular control. Asterisks refer to the control sample, indicating statistical significance (*$p < 0.05$; **$p < 0.01$) by Student's *t*-test. Data represent the mean ± standard deviation of three independent experiments. (**C**) Downregulation of EGFR-HA by EDEM1-Flag is mediated by the proteasome. HeLa cells were transfected with EGFR-HA (lane 1) or EGFR-HA and EDEM1-Flag (lanes 2 and 3). In co-transfected cells, cells were treated with MG132 (lane 3). Proteins were detected by western blotting with indicated antibodies. (**D**) Quantification of (C). Protein bands in (C) were quantified and plotted. Asterisks refer to the control sample, indicating statistical significance (N.S., not significant; **$p < 0.01$) by Student's *t*-test. Data represent the mean ± standard deviation of three independent experiments. (**E**) Physiological interaction of EDEM1-Flag and EGFR-HA. HeLa cells were co-transfected with EDEM1-Flag and EGFR-HA and part of the cell lysate (10%) was loaded as input (lanes 1–4), while the remaining lysate was used for immunoprecipitation for anti-Flag (lanes 5–8). Proteins were detected using indicated antibodies. In co-transfected cells, interaction of EDEM1-Flag and EGFR-HA was observed (lane 8).

 doi:10.20944/preprints202306.0751.v1

3. Discussion

The removal of terminally misfolded proteins from the ER is crucial for cell viability. This is because the accumulation of such misfolded proteins causes ER stress. Prolonged ER stress leads to apoptosis. Therefore, cells invoke UPR to recover from ER stress by enhancing protein folding and ERAD. EDEM1 is a gene induced by UPR that reinforces the degradation of misfolded proteins through ERAD. In this study, we showed that EDEM1 KD by siRNA induces the upregulation of XBP1s (an established UPR marker), and longer siRNA treatment leads to apoptosis. ER stress is associated with the development of numerous diseases, including breast cancer [28]. Hence, the management of ER stress *in vivo* offers promise for the treatment or prevention of such diseases.

The present analyses identified two clinically important molecules, namely TSP1 and EGFR, as the endogenous targets of EDEM1 for ERAD in HeLa cells. As both TSP1 and EGFR are intricated molecules, protein maturation of these molecules in the ER would be relatively difficult. It has been revealed that TSP1 forms a disulfide bond-mediated trimer and consists of structurally complex domains [29]. TSP1 is a matrix protein that can manage cell-cell communication and is required for angiogenesis. Therefore, it functions as a prognostic marker, particularly in breast cancer [30]. Research studies have highlighted the functional role of TSP1 in the development of diseases, including cancer [31,32].

EGFR is a well-established predictive biomarker in cancer. It is widely accepted that the overproduction of EGFR and mutation of the EGFR gene strongly affect several types of cancer [28]. Protein turnover and lysosomal degradation of EGFR after activation by binding of the extracellular ligand EGF has been well documented [33]. However, the protein maturation process of EGFR in the ER and the subsequent membrane trafficking to the plasma membrane have not been adequately addressed. Moreover, at present, there is limited information regarding the formation of the disulfide bonds of EGFR, the type of isomerases in the ER, and the type of ER-resident chaperone required for EGFR folding and assembly. A comprehensive analysis using a mass spectrometry-based capturing assay revealed that EDEM1 is an EGFR-associated protein [34]. This analysis supports our results suggesting the physiological interaction of EGFR with EDEM1 and EDEM1-mediated degradation of EGFR by ERAD. EDEM1 acts on misfolded proteins only during the maturation process in the ER. Thus, EDEM1 may exert a limited effect on the regulation of EGFR or TSP1 protein expression. Nevertheless, our results may assist in understanding the mechanisms underlying the effects of these clinically important molecules on protein biosynthesis and maturation.

Silencing of the EDEM1 gene suppresses the degradation of different ERAD substrates [35–38]. Of note, we found that the aggregation and turnover of lysosomal associated membrane protein 1 (Lamp1) and Lamp2a (lysosomal transmembrane proteins) were not significantly affected by EDEM1 KD (Figure S4), though it led to the aggregation of EGFR and TSP1 (Figs. 3–5). These findings suggested that EDEM1 is endowed with substrate specificity for ERAD. The three isoforms EDEM1, EDEM2, and EDEM3 differ in tissue distribution, expression levels, and membrane topology; EDEM1 is a soluble and type II membrane-anchored form, while EDEM2 and EDEM3 are soluble [21,39–41]. Thus, EDEM1–3 should be assigned ERAD substrate specificity since the ERAD pathway involves various secretory and membrane proteins.

It has been demonstrated that some secretory or membrane proteins require specific ER proteins for maturation or ERAD. Using such proteins as a model substrate, the precise role and mechanism of ERQC has been explored. ER-resident glucosidases UGGT1 and UGGT2 recognize and reglucosylate mal-folded secretory/membrane proteins to be returned into the lectin chaperone folding process termed the CNX cycle [25]. Endogenous targets which contain characteristic structural motifs for UGGT1 and UGGT2 have been previously identified [42]. The HSP90-like ER chaperone GRP94 targets γ-aminobutyric acid type A (GABAA) receptors as an endogenous ERAD substrate [43]. In addition, OS-9 (an ERAD component associated with the SEL1L/Hrd1 complex [44]), is the target of GRP94-mediated ERAD [45]. In the present study, we propose a novel aspect of EDEM1; at basal levels (i.e., not induced by UPR), EDEM1 acts on EGFR and TSP1 for ERAD. Analysis using endogenously but not exogenously expressed proteins provides a more natural aspect of the productive protein pathway and ERAD in cells and *in vivo*. The combination of an inductive approach

 doi:10.20944/preprints202306.0751.v1

and comprehensive analyses could be effective for understanding the detailed ERQC mechanism and role in physiology.

4. Materials and Methods

4.1. Antibodies, materials, and plasmids

Rabbit polyclonal anti-BiP, anti-ERp57, anti-CNX, and anti-CRT antibodies were kindly provided by Dr. Tetsuro Yamashita (Iwate University, Morioka, Japan). Rabbit polyclonal anti-CHOP (15204-1-AP; Proteintech) and rabbit monoclonal anti-EGFR (#4267; CST Japan) antibodies were purchased. Mouse monoclonal anti-ERp19 (Santa Cruz Biotechnology), anti-UGGT1 (Santa Cruz Biotechnology), anti-TSP1 (Santa Cruz Biotechnology), anti-Lamp1 (Santa Cruz Biotechnology), anti-Lamp2a (Santa Cruz Biotechnology), anti-αTubulin (Sigma), anti-Flag (Sigma), anti-HA (MBL Japan), anti-KDEL (MBL Japan), and rat anti-HA (7C9; Proteintech) antibodies were also purchased. For transfection and cellular protein expression analysis, plasmid vectors were generated as follows. The pCX4-bsr-EDEM1-Flag expressing C-terminal Flag-tagged EDEM1 was subcloned from the pEDEM1-3XFlag vector [20] through standard polymerase chain reaction (PCR) and cloning methods into the HpaI and NotI sites of pCX4-bsr. pCMV-EGFR-HA expressing C-terminal HA-tagged EGFR was generated by standard reverse transcription-PCR (RT-PCR) and PCR. Plasmids encoding NHK-Turquoise were provided by Dr. Ikuo Wada (Fukushima Medical University, Fukushima, Japan). Plasmids expressing CD10 C143Y-Flag were previously cloned and characterized [22]. The primers used for DNA cloning are included in Table 1.

4.2. Cell culture, transfection, siRNA, and RT-PCR

HeLa cells used in our previous study [22] were cultured in Dulbecco's modified Eagle's medium containing 10% fetal bovine serum and 1% penicillin/streptomycin in an incubator at 37°C, with 5% CO_2 and constant humidity. The cells were transfected with Fugene HD (Roche) according to the instructions provided by the manufacturer. The siRNA experiment was performed with RNAiMAX (Invitrogen) for 72 or 96 h according to the instructions provided by the manufacturer. Gene expression was verified by RT-PCR using reverse transcriptase Superscript II (Nippongene) and DNA polymerase Phusion (New England Biolabs) based on standard protocols. The primers used for RT-PCR and siRNA in this study are shown in Table 1.

4.3. Cell lysis, pulldown experiments, and western blotting

Proteins were extracted with 1% Triton X100-containing lysis buffer: 50 mM HEPES (pH: 7.5); 150 mM NaCl; 10 mM glucose; 2 units/ml hexokinase (Sigma); and protease inhibitor cocktails. The cells were collected and centrifuged at 4°C for 10 min. Subsequently, the cell lysate was denatured at 90°C for 5 min after the addition of 1% sodium dodecyl sulfate (SDS) and 1 mM dithiothreitol. For pulldown experiments, the cell lysate was treated using anti-Flag agarose beads (Sigma), as previously described [22]. Protein samples were subjected to reducing SDS-polyacrylamide gel electrophoresis (SDS-PAGE) and subsequently transferred onto a polyvinylidene difluoride membrane (Millipore). The membrane was blocked with tris-buffered saline containing 5% skim milk and 0.05% Tween 20 (Nacalai, Japan) at 4°C overnight. Next, the proteins were detected using indicated primary antibodies and secondary antibodies. Finally, they were visualized with enhanced chemiluminescence and the ChemiDoc system (Bio-Rad). Densitometric analysis was performed using the ImageJ software version 1.53 (National Institute of Health, Bethesda, MD, USA). The expression of proteins of interest was normalized to that of αTubulin. The error bars in figures represent the standard deviation for at least three independent experiments.

4.4. Glycosidase digestion

Treatment of denatured cellular proteins with Endo H and peptide-N-glycosidase F (PNGase F), both purchased from New England Biolabs, was conducted as previously described [46]. Total

cellular protein extracted using the aforementioned lysis buffer was denatured in the presence of Nonidet P-40. Subsequently, the samples were resolved by SDS-PAGE and analyzed using western blotting.

4.5. Indirect immunostaining

HeLa cells were seeded in a 35-mm dish. This was followed by transfection or siRNA treatment as indicated in the figure legends. After fixation using 4% paraformaldehyde in phosphate-buffered saline (PBS; Wako) at room temperature for 10 min, cells were incubated with 0.1% Triton X-100 in immunostaining buffer (PBS containing 1% goat serum (Gibco) and 5% glycerol) at 2°C for 1 min for membrane permeabilization. Fixation using methanol was conducted as follows. After addition of ice-cold methanol and incubation at −20°C for 10 min, the transfected cells were washed with PBS and blocked with the immunostaining buffer at room temperature for 5 min. Next, the cells were incubated with indicated primary antibodies and secondary antibodies, and stained with 4′,6-diamidino-2-phenylindole (DAPI; Wako) at room temperature for 5 min. The coverslip was washed with distilled water, placed on the slide, and fixed with Mowiol (Sigma). Confocal imaging was conducted with the LSM780 microscope (Zeiss).

Supplementary Materials: The following supporting information can be downloaded at the website of this paper posted on Preprints.org. **Figure S1. Knockdown of EDEM1 suppressed ERAD of misfolded proteins in HeLa cells.** Examination of ERAD after treatment of HeLa cells with siRNA against EDEM1. (**A**) HeLa cells were treated with siRNA for negative control (luciferase, Luc.) or EDEM1#1 for 24 h and subsequently transfected with CD10 C143Y-Flag for 48 h (total duration of siRNA treatment: 72 h). Cell lysates were resolved by western blotting using anti-Flag (for CD10 C143Y) or anti-αTubulin antibodies. (**B**) HeLa cells were treated with siRNA for negative control (luciferase, Luc.) or EDEM1#1 for 24 h, and transfected with NHK-Turquoise for 48 h (total duration of siRNA treatment: 72 h). Cell lysates were fractionated into supernatant (S) and precipitation (P) as detergent-insoluble proteins. NHK-Turquoise and αTubulin were detected with indicated antibodies. **Figure S2. Knockdown of EDEM1 did not result in accumulation of CNX and UGGT1.** HeLa cells were incubated with siRNA for negative control (luciferase, Luc.) or EDEM1#1 for 72 h. After fixation, indirect immunostaining using anti-CNX and anti-KDEL (**A**) or anti-ERp57 and anti-UGGT1 (**B**) antibodies was conducted. Anti-CNX and anti-ERp57 were visualized with Alexa Fluor 488 (green), while anti-KDEL and anti-UGGT1 were visualized with Alexa Fluor 594 (magenta). Images were obtained using confocal laser microscopy (LSM780; Zeiss). Merged images after DAPI staining and scale bars (represent 10 μm) are shown in panels c and f. **Figure S3. Solubility of Lamp1 and Lamp2a was not affected by knockdown of EDEM1.** HeLa cells were treated with siRNA for control or EDEM1 (Figure 4A). After the separation of the cell lysate into supernatant (S) and precipitation (P) fractions, Lamp1 (**A**) and Lamp2a (**C**) were detected by western blotting with indicated antibodies. Each corresponding band was quantified, and the levels were normalized to those of αTubulin (**B**) and (**D**). Asterisks refer to the control sample, indicating statistical significance (N.S., not significance) by Student's *t*-test. Data represent the mean ± standard deviation of three independent experiments. **Figure S4. Cellular trafficking of EGFR-HA co-expressed with EDEM1-Flag.** Immunocytochemistry of HeLa cells transfected with EGFR-HA with pcDNA (empty vector, upper panel) or EDEM1-Flag (bottom panel) for 48 h was performed. Anti-HA for EGFR-HA was visualized with Alexa Fluor 488 (green). Anti-Flag for EDEM1-Flag was visualized with Alexa Fluor 594 (magenta). Images were obtained using confocal laser microscopy (LSM780; Zeiss). Merged images after DAPI staining and scale bars (represent 10 μm) are shown in panels c and f.

Author Contributions: Kohta Miura, Riko Katsuki, Ren Ohta, Shusei Yoshida, and Taku Tamura performed the experiments; Kohta Miura and Taku Tamura analyzed the data and performed statistical analysis; Kohta Miura and Taku Tamura conceived and designed the experiments; Taku Tamura developed the experimental design and wrote the manuscript.

Acknowledgments: We greatly thank our laboratory members, including Nagisa Kato and Minori Ito, for their technical assistance and helpful discussion. We are grateful to Drs. Tetsuro Yamashita (Iwate University, Morioka, Japan), Ikuo Wada (Fukushima Medical University, Fukushima, Japan) and Dan Hebert (University of Massachusetts Amherst, Amherst, MA, USA) for providing materials used in this study. This research received no funding.

 doi:10.20944/preprints202306.0751.v1

Abbreviations

BiP	immunoglobulin-binding protein
CHOP	CCAAT-enhancer-binding protein homologous protein
CNX	calnexin
CRT	calreticulin
DAPI	4′,6-diamidino-2-phenylindole
EGFR	epidermal growth factor receptor
ER	endoplasmic reticulum
ERAD	endoplasmic reticulum-associated degradation
EDEM1	ER degradation-enhancing α mannosidase-like 1 protein
Endo H	endoglycosidase H
GAPDH	glyceraldehyde-3-phosphate dehydrogenase
NHK	α1 antitrypsin null Hong Kong
PNGase F	peptide N glycosidase F
siRNA	small interfering RNA
TSP1	thrombospondin-1
UGGT1	UDP-glucose:glycoprotein glucosyltransferase 1
WT	wildtype

References

1. Wiseman, R.L.; Mesgarzadeh, J.S.; Hendershot, L.M. Review Reshaping Endoplasmic Reticulum Quality Control through the Unfolded Protein Response. *Mol. Cell* **2022**, *82*, 1477–1491, doi:10.1016/j.molcel.2022.03.025.
2. Olzmann, J.A.; Kopito, R.R.; Christianson, J.C. The Mammalian Endoplasmic Reticulum-Associated Degradation System. *Cold Spring Harb. Perspect. Biol.* **2013**, *5*, doi:10.1101/cshperspect.a013185.
3. Slominska-Wojewodzka, M.; Sandvig, K. The Role of Lectin-Carbohydrate Interactions in the Regulation of ER-Associated Protein Degradation. *Molecules* 2015, *20*, 9816–9846.
4. Ninagawa, S.; George, G.; Mori, K. Mechanisms of Productive Folding and Endoplasmic Reticulum-Associated Degradation of Glycoproteins and Non-Glycoproteins. *Biochim. Biophys. Acta - Gen. Subj.* **2021**, *1865*, 129812, doi:10.1016/j.bbagen.2020.129812.
5. Sano, R.; Reed, J.C. ER Stress-Induced Cell Death Mechanisms. *Biochim. Biophys. Acta - Mol. Cell Res.* **2013**, *1833*, 3460–3470, doi:10.1016/j.bbamcr.2013.06.028.
6. Bhattacharya, A.; Qi, L. ER-Associated Degradation in Health and Disease - From Substrate to Organism. *J. Cell Sci.* **2019**, *132*, doi:10.1242/jcs.232850.
7. Kumari, D.; Brodsky, J.L. The Targeting of Native Proteins to the Endoplasmic Reticulum-Associated Degradation (Erad) Pathway: An Expanding Repertoire of Regulated Substrates. *Biomolecules* 2021, *11*.
8. Hwang, J.; Qi, L. Quality Control in the Endoplasmic Reticulum: Crosstalk between ERAD and UPR Pathways. *Trends Biochem. Sci.* 2018, *43*, 593–605.
9. Bhattacharya, A.; Sun, S.; Wang, H.; Liu, M.; Long, Q.; Yin, L.; Kersten, S.; Zhang, K.; Qi, L. Hepatic Sel1L-Hrd1 ER-associated Degradation (ERAD) Manages FGF21 Levels and Systemic Metabolism via CREBH. *EMBO J.* **2018**, *37*, doi:10.15252/embj.201899277.
10. Xu, L.; Liu, X.; Peng, F.; Zhang, W.; Zheng, L.; Ding, Y.; Gu, T.; Lv, K.; Wang, J.; Ortinau, L.; et al. Protein Quality Control through Endoplasmic Reticulum-Associated Degradation Maintains Haematopoietic Stem Cell Identity and Niche Interactions. *Nat. Cell Biol.* **2020**, *22*, 1162–1169, doi:10.1038/s41556-020-00581-x.
11. Bhattacharya, A.; Wei, J.; Song, W.; Gao, B.; Tian, C.; Wu, S.A.; Wang, J.; Chen, L.; Fang, D.; Qi, L. SEL1L-HRD1 ER-Associated Degradation Suppresses Hepatocyte Hyperproliferation and Liver Cancer. *iScience* **2022**, *25*, 105183, doi:10.1016/j.isci.2022.105183.
12. Shaukat, I.; Bakhos-Douaihy, D.; Zhu, Y.; Seaayfan, E.; Demaretz, S.; Frachon, N.; Weber, S.; Kömhoff, M.; Vargas-Poussou, R.; Laghmani, K. New Insights into the Role of Endoplasmic Reticulum-Associated Degradation in Bartter Syndrome Type 1. *Hum. Mutat.* **2021**, *42*, 947–968, doi:10.1002/humu.24217.
13. Tyler, R.E.; Pearce, M.M.P.; Shaler, T.A.; Olzmann, J.A.; Greenblatt, E.J.; Kopito, R.R. Unassembled CD147 Is an Endogenous Endoplasmic Reticulum-Associated Degradation Substrate. *Mol. Biol. Cell* **2012**, *23*, 4668–4678, doi:10.1091/mbc.E12-06-0428.
14. Huang, E.Y.; To, M.; Tran, E.; Lorraine, T.A.D.; Cho, H.J.; Baney, K.L.M.; Pataki, C.I.; Olzmann, J.A. A VCP Inhibitor Substrate Trapping Approach (VISTA) Enables Proteomic Profiling of Endogenous ERAD Substrates. *Mol. Biol. Cell* **2018**, *29*, 1021–1030, doi:10.1091/mbc.E17-08-0514.

15. Munteanu, C.V.A.; Chiritoiu, G.N.; Chiritoiu, M.; Ghenea, S.; Petrescu, A.J.; Petrescu, S.M. Affinity Proteomics and Deglycoproteomics Uncover Novel Edem2 Endogenous Substrates and an Integrative Erad Network. *Mol. Cell. Proteomics* **2021**, *20*, 0–21, doi:10.1016/j.mcpro.2021.100125.
16. Hosokawa, N.; Wada, I.; Hasegawa, K.; Yorihuzi, T.; Tremblay, L.O.; Herscovics, A.; Nagata, K. A Novel ER α-Mannosidase-like Protein Accelerates ER-Associated Degradation. *EMBO Rep.* **2001**, *2*, 415–422, doi:10.1093/embo-reports/kve084.
17. Shenkman, M.; Ron, E.; Yehuda, R.; Benyair, R.; Khalaila, I.; Lederkremer, G.Z. Mannosidase Activity of EDEM1 and EDEM2 Depends on an Unfolded State of Their Glycoprotein Substrates. *Commun. Biol.* **2018**, *1*, doi:10.1038/s42003-018-0174-8.
18. George, G.; Ninagawa, S.; Yagi, H.; Furukawa, J.; Hashii, N.; Ishii-Watabe, A.; Deng, Y.; Matsushita, K.; Ishikawa, T.; Mamahit, Y.P.; et al. Purified EDEM3 or EDEM1 Alone Produces Determinant Oligosaccharide Structures from M8B in Mammalian Glycoprotein ERAD. *Elife* **2021**, *10*, 70357, doi:10.7554/eLife.
19. Lamriben, L.; Oster, M.E.; Tamura, T.; Tian, W.; Yang, Z.; Clausen, H.; Hebert, D.N. EDEM1's Mannosidase-like Domain Binds ERAD Client Proteins in a Redox-Sensitive Manner and Possesses Catalytic Activity. *J. Biol. Chem.* **2018**, *293*, 13932–13945, doi:10.1074/jbc.RA118.004183.
20. Cormier, J.H.; Tamura, T.; Sunryd, J.C.; Hebert, D.N. EDEM1 Recognition and Delivery of Misfolded Proteins to the SEL1L-Containing ERAD Complex. *Mol. Cell* **2009**, *34*, doi:10.1016/j.molcel.2009.05.018.
21. Tamura, T.; Cormier, J.H.; Hebert, D.N. Characterization of Early EDEM1 Protein Maturation Events and Their Functional Implications. *J. Biol. Chem.* **2011**, *286*, 24906–24915, doi:10.1074/jbc.M111.243998.
22. Kanuka, M.; Ouchi, F.; Kato, N.; Katsuki, R.; Ito, S.; Miura, K.; Hikida, M.; Tamura, T. Endoplasmic Reticulum Associated Degradation of Spinocerebellar Ataxia-Related CD10 Cysteine Mutant. *Int. J. Mol. Sci.* **2020**, *21*, 1–19, doi:10.3390/ijms21124237.
23. Zinszner, H.; Kuroda, M.; Wang, X.Z.; Batchvarova, N.; Lightfoot, R.T.; Remotti, H.; Stevens, J.L.; Ron, D. CHOP Is Implicated in Programmed Cell Death in Response to Impaired Function of the Endoplasmic Reticulum. *Genes Dev.* **1998**, *12*, 982–995, doi:10.1101/gad.12.7.982.
24. Jeong, W.; Lee, D.Y.; Park, S.; Rhee, S.G. ERp16, an Endoplasmic Reticulum-Resident Thiol-Disulfide Oxidoreductase: Biochemical Properties and Role in Apoptosis Induced by Endoplasmic Reticulum Stress. *J. Biol. Chem.* **2008**, *283*, 25557–25566, doi:10.1074/jbc.M803804200.
25. Tannous, A.; Patel, N.; Tamura, T.; Hebert, D.N. Reglucosylation by UDP-Glucose: Glycoprotein Glucosyltransferase 1 Delays Glycoprotein Secretion but Not Degradation. *Mol. Biol. Cell* **2015**, *26*, 390–405, doi:10.1091/mbc.E14-08-1254.
26. Carlson, C.B.; Lawler, J.; Mosher, D.F. Thrombospondins: From Structure to Therapeutics - Structures of Thrombospondins. *Cell. Mol. Life Sci.* **2008**, *65*, 672–686, doi:10.1007/s00018-007-7484-1.
27. Tan, K.; Duquette, M.; Liu, J.H.; Dong, Y.; Zhang, R.; Joachimiak, A.; Lawler, J.; Wang, J.H. Crystal Structure of the TSP-1 Type 1 Repeats: A Novel Layered Fold and Its Biological Implication. *J. Cell Biol.* **2002**, *159*, 373–382, doi:10.1083/jcb.200206062.
28. Li, X.; Zhao, L.; Chen, C.; Nie, J.; Jiao, B. Can EGFR Be a Therapeutic Target in Breast Cancer? *Biochim. Biophys. Acta - Rev. Cancer* **2022**, *1877*, 188789, doi:10.1016/j.bbcan.2022.188789.
29. Chen, H.; Herndon, M.E.; Lawler, J. *The Cell Biology of Thrombospondin-1*; 2000; Vol. 19;.
30. Sun, S.; Dong, H.; Yan, T.; Li, J.; Liu, B.; Shao, P.; Li, J.; Liang, C. Role of TSP-1 as Prognostic Marker in Various Cancers: A Systematic Review and Meta-Analysis. *BMC Med. Genet.* 2020, *21*.
31. Kaur, S.; Bronson, S.M.; Pal-Nath, D.; Miller, T.W.; Soto-Pantoja, D.R.; Roberts, D.D. Functions of Thrombospondin-1 in the Tumor Microenvironment. *Int. J. Mol. Sci.* 2021, *22*.
32. Kale, A.; Rogers, N.M.; Ghimire, K. Thrombospondin-1 Cd47 Signalling: From Mechanisms to Medicine. *Int. J. Mol. Sci.* 2021, *22*.
33. Bakker, J.; Spits, M.; Neefjes, J.; Berlin, I. The EGFR Odyssey - from Activation to Destruction in Space and Time. *J. Cell Sci.* **2017**, *130*, 4087–4096, doi:10.1242/jcs.209197.
34. Yao, Z.; Darowski, K.; St-Denis, N.; Wong, V.; Offensperger, F.; Villedieu, A.; Amin, S.; Malty, R.; Aoki, H.; Guo, H.; et al. A Global Analysis of the Receptor Tyrosine Kinase-Protein Phosphatase Interactome. *Mol. Cell* **2017**, *65*, 347–360, doi:10.1016/j.molcel.2016.12.004.
35. Molinari, M.; Calanca, V.; Galli, C.; Lucca, P.; Paganetti, P. Role of EDEM in the Release of Misfolded Glycoproteins from the Calnexin Cycle. *Science (80-.).* **2003**, *299*, 1397–1400, doi:10.1126/science.1079474.
36. Papaioannou, A.; Higa, A.; Jégou, G.; Jouan, F.; Pineau, R.; Saas, L.; Avril, T.; Pluquet, O.; Chevet, E. Alterations of EDEM1 Functions Enhance ATF6 Pro-Survival Signaling. *FEBS J.* **2018**, *285*, 4146–4164, doi:10.1111/febs.14669.
37. Saeed, M.; Suzuki, R.; Watanabe, N.; Masaki, T.; Tomonaga, M.; Muhammad, A.; Kato, T.; Matsuura, Y.; Watanabe, H.; Wakita, T.; et al. Role of the Endoplasmic Reticulum-Associated Degradation (ERAD) Pathway in Degradation of Hepatitis C Virus Envelope Proteins and Production of Virus Particles. *J. Biol. Chem.* **2011**, *286*, 37264–37273, doi:10.1074/jbc.M111.259085.

38. Ron, E.; Shenkman, M.; Groisman, B.; Izenshtein, Y.; Leitman, J.; Lederkremer, G.Z. Bypass of Glycan-Dependent Glycoprotein Delivery to ERAD by up-Regulated EDEM1. *Mol. Biol. Cell* **2011**, *22*, 3945–3954, doi:10.1091/mbc.E10-12-0944.
39. Olivari, S.; Galli, C.; Alanen, H.; Ruddock, L.; Molinari, M. A Novel Stress-Induced EDEM Variant Regulating Endoplasmic Reticulum-Associated Glycoprotein Degradation. *J. Biol. Chem.* **2005**, *280*, 2424–2428, doi:10.1074/jbc.C400534200.
40. Mast, S.W.; Diekman, K.; Karaveg, K.; Davis, A.; Sifers, R.N.; Moremen, K.W. Human EDEM2, a Novel Homolog of Family 47 Glycosidases, Is Involved in ER-Associated Degradation of Glycoproteins. *Glycobiology* **2005**, *15*, 421–436, doi:10.1093/glycob/cwi014.
41. Hirao, K.; Natsuka, Y.; Tamura, T.; Wada, I.; Morito, D.; Natsuka, S.; Romero, P.; Sleno, B.; Tremblay, L.O.; Herscovics, A.; et al. EDEM3, a Soluble EDEM Homolog, Enhances Glycoprotein Endoplasmic Reticulum-Associated Degradation and Mannose Trimming. *J. Biol. Chem.* **2006**, *281*, 9650–9658, doi:10.1074/jbc.M512191200.
42. Adams, B.M.; Canniff, N.P.; Guay, K.P.; Larsen, I.S.B.; Hebert, D.N. Quantitative Glycoproteomics Reveals Cellular Substrate Selectivity of the Er Protein Quality Control Sensors Uggt1 and Uggt2. *Elife* **2020**, *9*, 1–27, doi:10.7554/ELIFE.63997.
43. Di, X.J.; Wang, Y.J.; Han, D.Y.; Fu, Y.L.; Duerfeldt, A.S.; Blagg, B.S.J.; Mu, T.W. Grp94 Protein Delivers γ-Aminobutyric Acid Type A (GABAA) Receptors to Hrd1 Protein-Mediated Endoplasmic Reticulumassociated Degradation. *J. Biol. Chem.* **2016**, *291*, 9526–9539, doi:10.1074/jbc.M115.705004.
44. Christianson, J.C.; Shaler, T.A.; Tyler, R.E.; Kopito, R.R. OS-9 and GRP94 Deliver Mutant A1-Antitrypsin to the Hrd1-SEL1L Ubiquitin Ligase Complex for ERAD. *Nat. Cell Biol.* **2008**, *10*, 272–282, doi:10.1038/ncb1689.
45. Dersh, D.; Jones, S.M.; Eletto, D.; Christianson, J.C.; Argon, Y. OS-9 Facilitates Turnover of Nonnative GRP94 Marked by Hyperglycosylation. *Mol. Biol. Cell* **2014**, *25*, 2220–2234, doi:10.1091/mbc.E14-03-0805.
46. Tamura, T.; Arai, S.; Nagaya, H.; Mizuguchi, J.; Wada, I. Stepwise Assembly of Fibrinogen Is Assisted by the Endoplasmic Reticulum Lectin-Chaperone System in HepG2 Cells. *PLoS One* **2013**, *8*, doi:10.1371/journal.pone.0074580.